Direct Measurement of the Percolation Probability in Carbon Nanofiber-Polyimide Nanocomposites

A. Trionfi,[1,*] D. H. Wang,[2] J. D. Jacobs,[2] L.-S. Tan,[2] R. A. Vaia,[2] and J. W. P. Hsu[1,†]

[1]*Sandia National Laboratories, Albuquerque, New Mexico 87185, USA*

[2]*Air Force Research Laboratory, Wright-Patterson AFB, Ohio 45433, USA*

(Received 21 November 2008; published 18 March 2009)

We present the first experimental measurement of the geometric critical exponent β associated with the percolation probability, the probability a metallic filler belongs to the conducting network, of an electrical composite. The technique employs conducting-tip atomic force microscopy to obtain a conducting areal density, and is demonstrated on polyimide nanocomposites containing different concentrations of carbon nanofibers. We find $\beta \approx 1$ and t (the exponent for bulk conductivity) ≈ 3. These values are consistent with the predictions for the Bethe lattice and larger than the values predicted in the 3D lattice percolation model. Hence, this electrical composite likely belongs to the same universality class as the Bethe lattice. The ability to measure geometric and transport critical exponents on the same material is critical to drawing this conclusion.

DOI: 10.1103/PhysRevLett.102.116601 PACS numbers: 72.80.Tm, 07.79.Lh, 81.05.Qk, 85.35.Kt

When a metallic phase is randomly dispersed in an insulating matrix, the resulting composite typically has a bulk electrical conductivity well described by percolation theory. Above the critical volume fraction (p_c) of the metallic phase, the bulk conductivity $\sigma(p)$ has been shown to take the form [1]

$$\sigma(p) \propto (p - p_c)^t \qquad (p > p_c), \tag{1}$$

where p is the volume fraction of the conducting phase, p_c is the percolation threshold, and t is the critical exponent. As with many second order phase transitions, the critical exponents associated with percolation theory, including t, are predicted to have universal values dependent only on the dimensionality of the system. In a 3D composite, the lattice percolation model predicts the critical exponent t to take a value of ≈ 2 [1]. It has been experimentally observed that the value of t deviates from this predicted value in many 3D percolation systems [2–6]. Theoretical explanations for the observed nonuniversal values of t focus on the contacts between adjacent particles. Explanations include low conductance bonds between conducting particles [7,8] and an extension of this idea to include tunneling conduction between nearest neighbor particles [9]. While these theories are able to explain nonuniversal t values, they cannot conclude the broad applicability of lattice percolation theory to 3D random network composites based on the result of t alone. This remains an unresolved problem of general interest in statistical physics.

In addition to t, percolation theory predicts other exponents, β, ν, and α associated with geometric properties of the conducting network: β is associated with the percolation probability $\theta_\infty(p)$, the probability a conducting particle belongs to the infinite cluster or conducting network; ν is associated with the correlation length ξ, the linear dimension of the largest metallic cluster not contributing to electrical transport; α is associated with the number of finite clusters in the system [10]. Experimental determination of these properties in electrical composites requires obtaining microscopic knowledge of the conducting network, as opposed to the bulk transport measurement needed to find t. A microscopic measurement would need the spatial resolution provided by microscopy techniques such as scanning electron microscopy (SEM), atomic force microscopy (AFM), and scanning tunneling microscopy. To the best of our knowledge, β, ν, or α has never been measured experimentally in an electrical composite. A measurement of any one of these critical exponents combined with an independent measurement of t should provide more in-depth insight into the cause of the nonuniversal behavior of t.

In this Letter, we report a direct experimental measurement of the percolation probability and its associated critical exponent β in carbon nanofiber loaded polyimide nanocomposites. The measurement employs the spatial resolution of the AFM by analyzing real-space conductance maps acquired using conducting-tip atomic force microscopy (CAFM). The development of CAFM and related electric force microscopy (EFM) has enabled the electrical properties of composite materials to be studied on the microscopic level to complement bulk transport measurements. The focus of past work in this area has included CAFM proof of concept studies [11,12] as well as EFM [13] and CAFM [14] studies of the fractal properties of a two phase carbon black composite. Here we use CAFM to image the conducting area (A_t) of a nanocomposite made of conducting multiwalled carbon nanofibers (CNF) dispersed in an insulating polyimide (CP2) matrix. The carbon nanofiber volume fractions in these samples are all above the percolation threshold. These nanocomposites exhibit a nonuniversal conductivity exponent t of ≈ 3 [15]. Details of the nanocomposite synthesis and characterization have been reported in Refs. [15–17].

To obtain $\theta_\infty(p)$ we employ a well-established identity of stereology known as the principle of Delesse (PoD). The PoD states that the areal density ($a_A = A_1/A_{\text{total}}$) of a phase in a random, isotropic, multiphase composite is equal to the volume density ($v_V = V_1/V_{\text{total}}$) of the phase assuming the measured area is representative of the bulk [18], where A_1 (V_1) are the area (volume) of the phase in the total measurement area, A_{total} (volume, V_{total}). This relationship is statistical so a good estimate of the volume density of a phase requires the average of many independent 2D areal densities. The PoD has been employed for many years analyzing optical images of biological specimens, but has not been widely applied in AFM image analysis [19]. In the case of CAFM imaging of an electrical composite, the conducting area in the image divided by the total scan area, A_t/L^2, tells us the areal density of the conducting network. If the total volume fraction of the conducting filler is known, then the ratio of the conducting areal density over the total volume fraction of the filler represents the fraction of the filler that is part of the conducting network, i.e., $\theta_\infty(p)$.

$$\theta_\infty(p) \propto (A_t/L^2)/p = C(p - p_c)^\beta \tag{2}$$

C is a constant. The lattice model predicts the value of β to be ≈ 0.4 in 3D [10].

In order for this composite material to be a candidate for the PoD analysis, it must be isotropic and have a uniform CNF dispersion. SEM and x-ray scattering measurements on these samples have turned up no detectable bulk anisotropy (i.e., no preferred CNF alignment). Therefore, we believe the bulk material is isotropic. Cross-sectional SEM images show uniform dispersion except for a polymer-rich surface layer. The amount of CNFs in the surface layer depends on whether the surface is exposed to air (top) or in contact with a glass substrate (bottom) during the synthesis process. The transition from surface to the bulk is sharp, within the resolution of the SEM. Prior to the CAFM measurements, the samples are removed from the glass substrate to create free-standing films and then etched in an oxygen plasma to remove $\approx$60 nm of the surface layer. Without such a treatment, the surfaces studied via CAFM would not be bulk representative, thus making the PoD analysis inapplicable [18]. After plasma etching, $\sigma(p)$ measured at different areas of each composite showed statistically similar values, further corroborating that nanotube dispersion is uniform across an 8×8 mm^2 sample [17]. Later we will show CAFM results suggesting that the surfaces produced by the oxygen plasma are bulk representative. The films we study are all over 100 μm thick while the average length of a CNF is about 8 μm and the average diameter is 80 nm. Any conducting pathways found in the material must be a part of a percolation network, as opposed to a single CNF spanning the entire thickness of the composites.

After the plasma treatment, a gold electrode was deposited via electron beam evaporation to cover one side of each sample. The CAFM measurements were performed with a Digital Instruments (DI) Dimension 3100 AFM with the extended TUNA module. Further details of the measurement setup can be found in Ref. [17]. CAFM scans over a 20×20 μm^2 area were taken at 24 randomly selected locations for each sample. A schematic of our CAFM measurement setup is shown in Fig. 1. Scan locations were selected randomly instead of pinning the origin of each scan to a conducting area as done in Refs. [13,14]. Therefore, the sum of the 24 scans should be statistically identical to a single scan with a square area of roughly 100 μm on the side. This is key because spurious results for A_t/L^2 can arise if the window size is less than the correlation length of the composite [13,14]. A study of a multiwalled carbon nanotube–epoxy composite found an estimate of $\approx$250 nm for the correlation length at loadings roughly 10 times higher than the percolation threshold of the material [20]. Even if the correlation length of this material is tens of microns near the percolation threshold, our measurement should still be sampling a homogeneous conducting network [21].

Example CAFM scans of composites with four different CNF loading are shown in Fig. 2. The bias voltage was 20, 50, 100, and 200 mV for the 0.035, 0.014, 0.007, and 0.0035 vol fractions, respectively. These voltages were set to maximize the current signal without pegging the CAFM current preamp. As shown previously [17], local current-voltage measurements on the conducting areas exhibit linear behavior, implying the different bias voltages are easily scalable to compare samples with different CNF loadings. The images depict spatial variation of current at a fixed tip-back contact bias. As is evident, most of the sample is not conducting (dark in the images), but isolated conducting areas do exist (bright in the images). Note that in order to detect a current signal, the AFM tip must contact a CNF that is in the conducting network because current must flow from the back Au contact through the sample to the tip. An isolated CNF in the insulating matrix will not produce a current signal. A_t was calculated by summing each pixel of a current map with a current signal above the 180 pA noise floor. The pixel count was then converted to an area by multiplying the total scan area divided by the total number of pixels in the scan. Scans shown were chosen that best represent the average A_t

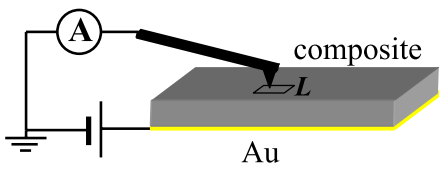

FIG. 1 (color online). Schematic of our CAFM measurement setup. A voltage bias is applied to the uniform bottom Au electrode while the CAFM tip is connected to ground through the TUNA current preamp. Multiple scans of size of $L = 20$ μm are taken at random locations for each CNF loading. Typical sample thickness is 150 μm with lateral dimensions of 8 mm.

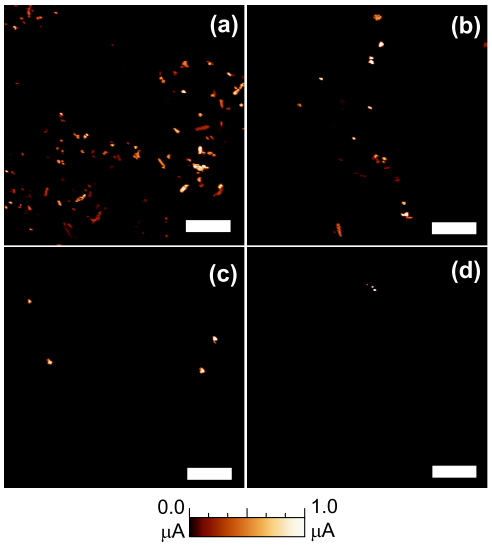

FIG. 2 (color online). Example CAFM scans of (a) 0.035, (b) 0.014, (c) 0.007, and (d) 0.0035 vol fraction CNF composites. Bias voltages were set at 20, 50, 100, and 200 mV for (a), (b), (c), and (d), respectively. In order to keep the current scale the same for all scans, the current magnitude of each pixel has been increased by a factor of 2, 10, and 20 for (b), (c), and (d), respectively. The white scale bar represents 4 μm.

measured for each loading. It is clear that A_t changes with the CNF concentration.

It was mentioned earlier that the CAFM measurements also facilitated a means to check whether the surfaces being measured are bulk-representative. On as-made 0.035 vol fraction materials, the A_t values for the surface exposed to air during synthesis and that in contact with glass during synthesis are 3.14 ± 1.33 μm^2 and 0.202 ± 0.114 μm^2 for 20×20 μm^2 scans, respectively. The difference is likely caused by the different surface energies experienced by the polyimide and CNFs at the two interfaces. After the plasma treatment, A_t measurements on both surfaces give statistically identical results; 21.9 ± 3.77 μm^2 on the glass-interface side and 21.6 ± 5.57 μm^2 on the air-interface side. These results strongly suggest that the plasma treatment removes polymer-rich skin layers and produces bulk-representative surfaces.

As shown in Eq. (2), once A_t has been measured for a series of scans, $\theta_\infty(p)$ can be estimated by dividing A_t/L^2 by p. Figure 3 shows the calculated $\theta_\infty(p)$ for all six CNF volume fractions. Using Eq. (2) to fit the data, we found the following values for β and p_c: 1.1 ± 0.3 and $0.002 \pm .002$ vol fraction. The inset of Fig. 3 shows the $\sigma(p)$ of each CNF loading. Using Eq. (1), we can independently determine p_c as well as verify the nonuniversal value of t seen in previous studies of this composite material [15]. The best fit from $\sigma(p)$ results gives a p_c value of 0.001 ± 0.001 vol fraction and a t value of 3.1 ± 0.4. It is important to point out that the two measurements probe different properties in the nanocomposites; as CNF loading increases, $\theta_\infty(p)$ measures the increase in the conducting network volume without regard to the conductivity amplitude, while $\sigma(p)$ measures how the average bulk conductivity increases. The fact that the values of p_c obtained from these two independent measurements agree within the uncertainty of the measurements gives us confidence that we have verified the percolation threshold of our composite system by the CAFM measurement. Hence, our A_t analysis is truly giving us the $\theta_\infty(p)$ behavior of these nanocomposites. The small p_c value is due to the high aspect ratio ($\approx$100) of the CNF fillers [22], and will be discussed further below within the context of the Bethe lattice. As given in the supplementary material [21], the measured $\theta_\infty(p)$ values are too large by a constant multiplicative factor due to AFM tip convolution and image pixilation. However, this multiplicative factor does not affect the resultant values of p_c or β obtained from the CAFM measurement.

It is clear that both critical exponents measured in our CNF composite ($t \approx 3$, $\beta \approx 1$) do not agree with the values predicted in the 3D lattice percolation model ($t \approx 2$, $\beta \approx 0.4$). The results bring into question the applicability, in our nanocomposite, of the contact (tunneling) models that were proposed to explain the nonuniversal values of t. This hinges upon the fact that while models such as the tunneling model suggest nonuniversal values for t, they predict the geometric critical exponents such as β should still be the same as that predicted by the lattice percolation model [23]. Since the β value we obtain for the CNF nanocomposites does not agree with the value predicted by the lattice model, the contact (tunneling) models are not applicable to this system. In addition, the fractal dimension D_f is related to the geometric critical exponents β and ν via the scaling law $D_f = d - \beta/\nu$ [10], where d is the Euclidean spatial dimension. The lattice model predicts a $D_f \approx 2.5$ with $\nu \approx 0.8$. Small angle x-ray scattering re-

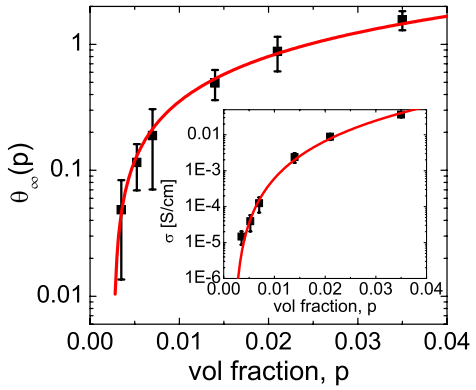

FIG. 3 (color online). The percolation probability as a function of CNF volume fraction for the CNF—polymer composite. The inset shows the bulk conductivity of the composite as a function of CNF volume fraction. The red line in both curves is a best fit to the data using the functional form $y = A(p - p_c)^z$. The critical exponent is 1.1 ± 0.3 for $\theta_\infty(p)$ and 3.1 ± 0.4 for $\sigma(p)$. The p_c value is 0.002 ± 0.001 vol fraction determined from $\theta_\infty(p)$ and 0.001 ± 0.001 vol fraction from $\sigma(p)$.

sults indicate $D_f \approx 2$ and, hence, $\nu \approx 1$ for our composite material [15]. Both are also different from the prediction of the lattice model. We are left to consider if this CNF-polyimide nanocomposite belongs to a different universality class than the 3D lattice percolation model.

The Bethe lattice (or a Cayley tree) is an endless branching network with no close loops [1,24]. This model is exactly solvable due to its unique topology, and has been applied to explain the gelation process. Curiously, $\beta = 1$ and $t = 3$ for the Bethe lattice, as we measured experimentally. To map our system to a Cayley tree, the nodes would correspond to CNFs while the bonds to CNF-CNF contacts. The number of bonds per node is z, the coordination number. The high aspect ratio of CNFs results in more contacts (bonds) per CNF (node). p_c in the Bethe lattice equals $(z-1)^{-1}$. In our system, p_c of 0.002 corresponds to $z \approx 500$, which is large but of the same order as the CNF aspect ratio. Thus, it appears that the electrical conduction in the CNF-polymer nanocomposites behaves similar to the Bethe lattice. However, it is not clear that having no loops in the cluster is an accurate description of the CNF network topology. Cross-sectional SEM images of our nanocomposite [21] show an entangled CNF distribution, implying loops cannot be precluded. Perhaps due to the stiffness of the CNFs and-or the high z value, forward-propagating branches dominate, rendering the loop contributions insignificant. While we cannot conclusively say that the CNF nanocomposites form a Bethe lattice, the agreement of the two critical exponents is highly suggestive.

In summary, we present the first experimental measurement of $\theta_\infty(p)$ in an electrical composite. Our approach is based on imaging conducting areas of bulk-representative cross sections using CAFM and applying the principle of Delesse. $\theta_\infty(p)$ is a geometric property, and while theoretical models are able to explain the nonuniversal transport critical exponent with varying contact resistances, nonuniversal geometric critical exponents, such as β, cannot be explained in the same way. We conclusively show that, by measuring t and β on the same samples, CNF-polyimide nanocomposites do not belong to the same universality class as the 3D lattice percolation model. Instead, their properties more closely resemble a Bethe lattice. This conclusion could not have been made without measuring both geometric and transport exponents. Thus, our development of an experimental approach to obtain β is critical. Our approach is clearly not limited to the CNF-polyimide nanocomposite system. It would be very interesting to investigate composites where the material properties suggest the tunneling percolation model is applicable, e.g., carbon black composites [14] and some granular metal composites [25]. It would also be informative to perform this measurement on systems with a t value that appears to be in agreement with the lattice model.

We would like to thank D. Schaefer, G. Beaucage, K. Lyo, and R. Fleming for useful discussion. This work was performed in part at the U.S. Department of Energy, Center for Integrated Nanotechnologies, at Los Alamos and Sandia National Laboratories. Sandia National Laboratories is a multiprogram laboratory operated by Sandia Corporation, a Lockheed-Martin Company, for the U.S. Department of Energy under Contract No. DE-AC04-94AL85000.

*trionfia@mailaps.org
†jwhsu@sandia.gov

[1] D. Stauffer and A. Aharony, *Introduction to Percolation Theory* (Taylor and Francis, London, 1992).
[2] D. S. McLachlan, M. Blaszkiewicz, and R. E. Newnham, J. Am. Ceram. Soc. **73**, 2187 (1990).
[3] S. I. Lee, Y. Song, T. W. Noh, X. D. Chen, and J. R. Gaines, Phys. Rev. B **34**, 6719 (1986).
[4] G. E. Pike, AIP Conf. Proc. **40**, 366 (1978).
[5] F. Carmona, P. Prudhon, and F. Barreau, Solid State Commun. **51**, 255 (1984).
[6] Other examples are listed in C. Brosseau, J. Appl. Phys. **91**, 3197 (2002).
[7] P. M. Kogut and J. P. Straley, J. Phys. C **12**, 2151 (1979).
[8] S. Feng, B. I. Halperin, and P. N. Sen, Phys. Rev. B **35**, 197 (1987).
[9] I. Balberg, Phys. Rev. Lett. **59**, 1305 (1987).
[10] C.-W. Nan, Prog. Mater. Sci. **37**, 1 (1993).
[11] E. Z. Luo, J. B. Xu, W. Wu, I. H. Wilson, B. Zhao, and X. Yan, Appl. Phys. A **66**, S1171 (1998).
[12] J. Planès, F. Houzé, P. Chrétien, and O. Schneegans, Appl. Phys. Lett. **79**, 2993 (2001).
[13] R. Viswanathan and M. B. Heaney, Phys. Rev. Lett. **75**, 4433 (1995).
[14] N. Shimoni, D. Azulay, I. Balberg, and O. Millo, Phys. Status Solidi (b) **230**, 143 (2002).
[15] M. J. Arlen, D. Wang, R. Justice, A. Trionfi, J. W. P. Hsu, D. Schaffer, L.-S. Tan, and R. A. Vaia, Macromolecules **41**, 8053 (2008).
[16] D. H. Wang, M. J. Arlen, J.-B. Baek, R. A. Vaia, and L.-S. Tan, Macromolecules **40**, 6100 (2007).
[17] A. Trionfi, D. A. Scrymgeour, J. W. P. Hsu, M. J. Arlen, D. J. Jacobs, D. Tomlin, L.-S. Tan, D. Wang, and R. A. Vaia, J. Appl. Phys. **104**, 083708 (2008).
[18] E. R. Weibel, *Stereological Methods* (Academic Press, San Diego, 1979), Vol. 1.
[19] M. Göken and M. Kempf, Acta Mater. **47**, 1043 (1999).
[20] G. Pécastaings, P. Delhaès, A. Derr, H. Saadaoui, F. Carmona, and S. Cui, J. Nanosci. Nanotechnol. **4**, 838 (2004).
[21] See EPAPS Document No. E-PRLTAO-102-049913 for further discussion. For more information on EPAPS, see http://www.aip.org/pubservs/epaps.html.
[22] A. Celzard, E. McRae, C. Deleuze, M. Dufort, G. Furdin, and J. F. Marêché, Phys. Rev. B **53**, 6209 (1996); X. Zhen, M. G. Gorest, R. Vaia, M. Arlen, and R. Zhou, Adv. Mater. **19**, 4038 (2007).
[23] I. Balberg, Phys. Rev. B **37**, 2391 (1988).
[24] J. P. Straley, J. Phys. C **10**, 3009 (1977).
[25] D. Toker, D. Azulay, N. Shimoni, I. Balberg, and O. Millo, Phys. Rev. B **68**, 041403(R) (2003).